J Neurophysiol 102: 2603–2615, 2009.
First published July 1, 2009; doi:10.1152/jn.91255.2008.

Organization of Hue Selectivity in Macaque V2 Thin Stripes

Heejin Lim,[1,*] Yi Wang,[1,2,*] Youping Xiao,[1,3,*] Ming Hu,[2] and Daniel J. Felleman[1]

[1]*Department of Neurobiology and Anatomy, University of Texas Medical School–Houston, Houston, Texas;* [2]*State Key Laboratory of Brain and Cognitive Sciences, Institute of Biophysics, Chinese Academy of Sciences, Beijing, China; and* [3]*Department of Neuroscience, Mount Sinai School of Medicine, New York, New York*

Submitted 25 November 2008; accepted in final form 28 June 2009

Lim H, Wang Y, Xiao Y, Hu M, Felleman DJ. Organization of hue selectivity in macaque V2 thin stripes. *J Neurophysiol* 102: 2603–2615, 2009. First published July 1, 2009. doi:10.1152/jn.91255.2008. V2 has long been recognized to contain functionally distinguishable compartments that are correlated with the stripelike pattern of cytochrome oxidase activity. Early electrophysiological studies suggested that color, direction/disparity, and orientation selectivity were largely segregated in the thin, thick, and interstripes, respectively. Subsequent studies revealed a greater degree of homogeneity in the distribution of response properties across stripes, yet color-selective cells were still found to be most prevalent in the thin stripes. Optical recording studies have demonstrated that thin stripes contain both color-preferring and luminance-preferring modules. These thin stripe color-preferring modules contain spatially organized hue maps, whereas the luminance-preferring modules contain spatially organized luminance-change maps. In this study, the neuronal basis of these hue maps was determined by characterizing the selectivity of neurons for isoluminant hues in multiple penetrations within previously characterized V2 thin stripe hue maps. The results indicate that neurons within the superficial layers of V2 thin stripe hue maps are organized into columns whose aggregated hue selectivity is closely related to the hue selectivity of the optically defined hue maps. These data suggest that thin stripes contain hue maps not simply because of their moderate percentage of hue-selective neurons, but because of the columnar and tangential organization of hue selectivity.

INTRODUCTION

Early electrophysiological studies of area V2 emphasized the segregation of receptive field properties in different cytochrome oxidase stripes. These studies suggested that thin stripes contained color-selective cells, interstripes contained orientation-selective cells, and thick stripes contained disparity and end-stopped cells (e.g., DeYoe and Van Essen 1985; Hubel and Livingstone 1987; Livingstone and Hubel 1988; Shipp and Zeki 2002). Subsequent investigations emphasized a greater homogeneity of neuronal properties across stripes, suggesting that orientation- and color-selective cells were found in nearly equal percentages across all three stripes (Gegenfurtner 2003; Gegenfurtner et al. 1996; Levitt et al. 1994; Shipp and Zeki 2002). In contrast to these electrophysiological findings, optical recordings of intrinsic cortical activity have consistently demonstrated color-preferring modules or hue maps only in thin stripes, orientation-selective modules in both thick and interstripes, and binocular disparity and direction maps only in thick stripes (e.g., Chen et al. 2008; Lu and Roe 2008; Roe and Ts'o 1995; Ts'o et al. 2001; Xiao et al. 2003). If the neuronal selectivity for color, orientation, direction, and/or disparity is largely homogeneous across V2 cytochrome oxidase stripe compartments, why are different feature maps localized to different stripe compartments?

In our previous study of spatially organized hue maps in V2, we demonstrated the correlation between neuronal and optical tuning for only a subset of recording sites centered within the hue map (Xiao et al. 2003). The objective of this study was to explore this relationship in multiple V2 thin stripes, both within and just outside the statistically significant peak hue map, using more sensitive quantitative techniques. These experiments focus on the relationships among single-neuron selectivity for hue, the average neuronal selectivity for hue within perpendicular penetrations, and neuronal population selectivity for hue as determined through intrinsic cortical optical imaging. We show that V2 thin stripes contain substantial percentages of hue-selective cells that are organized into iso-hue columns whose preferred hue shifts systematically across the cortical surface consistent with the optically defined hue maps.

METHODS

Optical recording

Optical recording of intrinsic cortical signals was carried out using methods described previously (Wang et al. 2007; Xiao et al. 2003). Briefly, three long-tailed macaque monkeys (*Macaca fascicularis*) were prepared for chronic optical and microelectrode recording by sterile implantation of a recording chamber over V2 of both hemispheres. A craniotomy and durectomy were performed to reveal portions of areas V1 and V2 adjacent to the lunate sulcus. The chamber was then filled with sterile silicone oil and sealed with an antireflection-coated glass lid. The cortical surface was illuminated with 605-nm light that was generated by a tungsten source (Zeiss) driven by an ultrastable power supply (Kepco) and delivered by fiber optics. The cortex was imaged using a cooled, slow-scan charge-coupled detector camera (Photometrics) using a dual-lens macroscope (Ratzlaff and Grinvald 1991). Images of cortex were acquired for 4 s at a rate of 2 frames/s, beginning 0.5 s prior to stimulation and lasting through the stimulation period. The resultant cortical response was captured in the ascending and plateau regions of the hemodynamic response, where four images were averaged to quantify the response. Single-condition responses were calculated as the deviation of the signal from the first, no-stimulus frame of each response.

Thin stripes were identified by *1*) their location in V2 as determined by the distinct ocular dominance pattern in V1 but not V2, *2*) their preferential activation to color in the differential image of red/green isoluminant versus achromatic luminance contrast gratings (e.g., Lu and Roe 2008) that was distinct from the regular arrays of "color blobs" in V1, *3*) the presence of systematic maps of hue (e.g., Xiao

* These authors contributed equally to this work.

Address for reprint requests and other correspondence: D. J. Felleman, Department of Neurobiology and Anatomy, University of Texas Medical School–Houston, 6431 Fannin St., Houston, TX 77030 (E-mail: daniel.felleman@uth.tmc.edu).

et al. 2003), and *4*) their lack of a spatially organized orientation map and the presence of such maps in the adjacent cortical domains (e.g., Wang et al. 2007; Xiao et al. 2003; see, e.g., Fig. 1*A*). However, despite these criteria and their application in other laboratories there still remains some controversy concerning the identification of V2 "thin stripes" (e.g., Sincich and Horton 2005). Perhaps these criteria can be enhanced, as they suggest, by applying color-exchange experiments that use stimuli equated for contrast and form and vary in chromatance (Wade et al. 2002).

The organization of the representation of isoluminant hue in V2 thin stripes was determined from single-condition images in response to isoluminant hue/gray gratings (0.25 cycle/deg at two alternating spatial phases; and four orientations; 0, 90, 45, and 135°) or homogeneous fields of a given hue (Xiao et al. 2003). A series of four to eight different hues were presented in random order and the optical responses were averaged over 50 repetitions of each hue. The location of each hue response was calculated from single-condition images that demonstrated the stimulus-induced response compared with the no-stimulus first-frame condition. The spatial representation of hue preference in V2 was determined by identifying, in each single-condition (hue) image, those pixels that demonstrated a statistically significant ($P < 0.005$) activation compared with the prestimulus background identified using a *t*-test. Next, the region of the statistically significant activation that exceeded 75% of the peak response was identified as the statistically significant peak response region for each hue. These significant peak response domains are identified by color-coded contours from each single-condition image that were then projected onto the cortical surface (see Figs. 2, *B* and *D* and 3, *A–D*; see Conway et al. 2007; Sincich and Horton 2005). This method was used to demonstrate the spatial organization of significant hue responses based on peak response magnitude, but is unable to encode the selectivity for hue across the cortical map.

Visual stimuli and data analysis

The spatial organization and selectivity for stimulus hue were analyzed using hue response maps. In this second method, the preferred hue and hue selectivity were calculated on a pixel-by-pixel basis using the vector-summation method, conventionally used to analyze orientation selectivity (e.g., Levick and Thibos 1982; Shou and Leventhal 1989), and has recently been applied to the analysis of hue selectivity (Conway et al. 2007). Similar to the angle applied to orientation selectivity calculations, each stimulus hue was assigned a color angle on the basis of their CIE 1976 Lu*v* color-space coordinates (Wyszecki and Stiles 1982). In this analysis, the following CIE-xy chromaticity and color angles for 10 cd/m^2 isoluminant stimuli were used: red, 0.55, 0.33, 14.8°; orange, 0.54, 0.40, 31.9°; yellow, 0.45, 0.47, 69.8°; green, 0.27, 0.49, 136.4°; aqua, 0.23, 0.36, 170.2°; blue, 0.16, 0.08, 264.6°; purple, 0.23, 0.11, 279.8°. The response to each stimulus was expressed as a vector at hue angle (θ) analogous to direction angle (Φ, 0–360°) and all vectors were summed and divided by the sum of the absolute values of the vectors, to define a bias vector whose magnitude varies from 0 (equal responses to all θ) to 1 (response to only one θ). The angle of the resultant bias vector corresponds to the cells' preferred hue. The resultant vector angles and magnitudes were represented as separate maps that were then multiplied to form the color vector response map. The resultant vector angles were mapped using the following look-up table: 327–22° = red; 22–50° = orange; 50–103° = yellow; 103–153° = green; 153–217° = aqua; 217–271° = blue; and 271–327° = purple. The degree of hue selectivity was encoded by the brightness of the resultant color; bright colors indicate high hue selectivity indicated by large vector magnitudes, whereas dim colors indicate low hue selectivity and small vector magnitudes.

Since the specific hues (color angles) were selected and used as test stimuli prior to the application of the vector-summation technique (e.g., Conway et al. 2007), their inhomogeneous distribution across this color space resulted in a small residual bias (0.11) that violated the assumption of zero bias for equal responses to all tested stimuli. Our efforts to systematically remove this residual vector produced unexpected, differential consequences on the neuronal and optical summed vectors. For the most part, most optical signals were positive for all tested color angles, so the subtraction of a specific vector tended to have the intended effect. However, for many of the neurons, near-zero responses were observed at many color angles, so the effect of subtracting the "residual" was to add a small vector in the opposite direction. Furthermore, the magnitude of this effect varied with the preferred color angle, thus further undermining this "residual" vector removal method.

Since the same residual was present in the vectorial representations of the optical and electrophysiological responses, comparisons of the resultant preferred color angles and summed vector magnitudes seemed appropriate. However, the statistical significance of these resultant vectors cannot be evaluated using traditional methods that evaluate the probability of the summed vector magnitude on the basis of the Rayleigh distribution (Fisher 1993; Mardia and Jupp 2000). Although a method to evaluate summed vectors resulting from inhomogeneous distributions of input vectors has been published (Swindale 1998), the resultant preferred angles and vector magnitudes did not appropriately capture the optical or electrophysiological response tuning (N. Swindale, personal communication). Therefore a bootstrap method was used to evaluate the statistical probability of our summed vector magnitudes. Synthetic summed vector magnitudes were generated using one fixed-peak response (normalized 1.0) and then assigning randomly selected input vector magnitudes chosen from the von Mises distribution (see Swindale 1998). This process was repeated 10,000 times and the vector magnitude representing the 5% cutoff ($P < 0.05$) was taken as the minimum significant vector magnitude. This bootstrap method resulted in a threshold vector magnitude criterion of 0.1836 (0.2490 for four orientations). Therefore summed vector magnitudes >0.1836 should be considered significant at the $P < 0.05$ level, whereas smaller vector magnitudes should be considered nonsignificant.

Each color's cone excitations were given by the dot product of the color's spectral power distribution and the cone fundamentals (Stockman and Sharpe 2000). L-M cone contrast was calculated by $\Delta L/L - \Delta M/M$, where $\Delta L/L$ and $\Delta M/M$ were the L and M cone contrast relative to the background, respectively. S cone contrast was calculated by $\Delta S/S$.

Electrophysiological recording

Microelectrode penetrations were directed to specific functionally defined loci under visual guidance through the clear aperture top of the hydraulically sealed recording chamber using a surgical microscope (×20–50). Paralene-C–coated tungsten microelectrodes (Z = 1–5 MΩ) were advanced into the cortex using a stepping motor microdrive. Neuronal signals were conventionally amplified (DAM 80, WPI) and fed into a time–amplitude window discriminator (BAK Electronics), which provided input to the data acquisition system (Discovery, DataWave Technology). A Silicon Graphics workstation (Indigo High Impact) presented calibrated static and moving stimuli within the recorded cell's receptive field.

Recording procedure

As the electrode was advanced into the cortex, bar stimuli were swept through the expected visual field location and neural activity was monitored. Search stimuli were varied in color, size, and orientation and single- or multiunit (two to three cells) receptive fields were then isolated. In general, stimuli just filled the hand-plotted receptive field. Data acquisition included tests for hue selectivity using flashed isoluminant hues (10 cd/m^2), flashed isoluminant hue/gray gratings (identical to the stimuli used in the optical recording experiments), or

moving isoluminant hue/gray gratings (1.5 c/d, 1 cycle/s). In each penetration, one to six single- or multiunit recording sites were assessed for hue selectivity. Data were analyzed by the mean response (response-spontaneous) during the full period of stimulus presentation (usually 1.28 s) for each hue across 10–20 repetitions. The responses were compiled as peristimulus time histograms and were displayed as conventional tuning curves (means ± SE) or vector plots of individual hue responses and the resultant summed vector.

RESULTS

The purpose of these experiments was to compare the organization and selectivity of V2 thin stripe hue maps to the selectivity for hue observed in individual cells and across perpendicular penetrations within thin stripes. In this section, the consistency of hue selectivity in a single microelectrode penetration is first illustrated. Then, the detailed results from one exemplary hemisphere are presented. Finally, the summary results comparing penetration average electrophysiological tuning with optical recording estimates of color tuning are described for two additional hemispheres. In these experiments, optical recording of intrinsic cortical signals is first used to identify orientation maps in V2 thick stripes and interstripes and to characterize the organization and selectivity for hue in V2 thin stripes. Next, electrophysiological recording is used to determine the hue selectivity of individual recording sites (single- and multiunit data) and these results are then averaged to determine the aggregate hue preference and hue selectivity of each penetration. Finally, the relationships of hue preference and hue selectivity are analyzed between individual recording sites, penetration average electrophysiological responses, and optical recording responses within a region of interest (ROI) centered at the site of each electrode penetration.

Hue selectivity within a single penetration

The neuronal selectivity for hue in a single penetration within the statistically significant peak response (75% maximal) portion of a V2 thin stripe is illustrated in Fig. 1. In agreement with previous studies, V2 thin stripes were identified by their lack of significant orientation selectivity , their preferential activation to chromatic stimuli, and the presence of spatially organized hue maps (e.g., Lu and Roe 2008; Wang et al. 2007; Xiao et al. 2003). In this experiment, a portion of V2 near the lip of the lunate sulcus was first imaged under green light to establish the pattern of cortical vasculature and V2 thick stripes and interstripes were identified by the presence of their highly selective maps of orientation (Fig. 1, *A* and *B*). The 1.5-mm gap in this orientation map was then identified as a thin stripe by its preferential activation to chromatic stimuli (not shown) and by the presence of a spatially organized hue map (Fig. 1, *C* and *D*). Microelectrodes were advanced into the cortex under visual guidance, using the surface vasculature as reference to the optically defined orientation- and color-selective domains (Fig. 1, *A* and *B*). Figure 1, *C* and *D* illustrates the location of one of these penetrations (penetration H) with respect to the hue map defined by the color-coded statistically significant ($P < 0.005$) peak responses to individual hues. The receptive fields of isolated cells were plotted on the face of the cathode-ray tube and stimuli were selected to fill the mapped receptive field of each neuron. An example vector response plot that indicates the color angles of the hues tested in this experiment is illustrated in Fig. 1*E*. The corresponding cone contrasts of the test stimuli are illustrated by the center of the color-coded bubble plots in Fig. 1*F*. The neuronal responses to each tested hue are plotted as conventional tuning curves (Fig. 1*G*), vector response plots (Fig. 1*H*), and cone-contrast (L-M vs. S-cone) bubble plots, in which the area of the bubble indicates the response to each stimulus (Fig. 1*I*). In Fig. 1*H*, the single-hue response vectors (black) are plotted as normalized response magnitudes at the corresponding color angle. The vector sum of these single-hue responses is illustrated as the red vector, which characterizes the cell's preferred hue (color angle) and hue selectivity (vector magnitude).

This penetration contained three highly selective single units that demonstrated peak responses to red or red-orange flashed stimuli. The first cell, recorded at a depth of about 400 μm, was maximally responsive to flashed isoluminant orange, with rapidly diminishing responses to green, aqua, and blue, which resulted in a high bias value of 0.572 (preferred angle = 38.14°). In this and subsequent figures, the responses at individual recording sites are coded as SS [single unit, static (flashed)], SM (single-unit isoluminant moving), MS (multiunit static), or MM (multiunit moving). The second cell, recorded 200 μm deeper, was highly selective for yellow flashed stimuli (bias = 0.656; preferred angle = 49.08°) and showed minimal responses to green-purple stimuli. The third cell was recorded at 720 μm and showed a peak response to yellow, but slightly greater responses to aqua-purple and red, which resulted in a slightly reduced hue selectivity (bias = 0.466), yet it retained a preferred color angle (41.82°) that was very consistent with that of the other two cells in the penetration. The average cell hue selectivity observed in this penetration was 0.564 and the average preferred color angle was 43.01° (Fig. 1*J*).

The penetration average hue tuning is illustrated in the conventional tuning curve, vector polar plot, and cone-contrast bubble plot in Fig. 1*K*. The average response peaked at yellow, with a minimum response to aqua, resulting in a statistically significant variation of response as a function of hue (ANOVA, $P < 0.003$). Similarly, the penetration average color vector plot was generated by averaging the vector magnitudes for each hue across the three cells in this penetration. The resulting summed color vector thus characterizes the preferred hue and hue selectivity of the column of cells recorded. The resultant penetration average vector was characterized by a preferred angle of 43.68° (orange) with a highly selective vector magnitude of 0.553 ($P < 0.001$).

Hue selectivity within multiple thin stripe penetrations

Seventeen electrode penetrations were directed at optically defined, color-preferring modules in V2 thin stripes in three macaque monkeys. In this section, the tuning properties of single cells and the average tuning properties of these cells are described in detail for one illustrative case. The penetration average tuning properties from eight penetrations from the other two cases are described in relation to their correlated optical tuning properties. In each penetration, one to five recording sites were analyzed for hue selectivity and the penetration average hue selectivity was characterized by its preferred color angle and summed vector magnitude (bias).

CASE M0103. The intrinsic cortical imaging map of preferred orientation in Fig. 1, *A* and *B* delineates the strong (bright colors) orientation-selective domains in V2 thick stripes and interstripes and the orientation-nonselective (dark) regions in a V2 thin stripe. Figure 1*B* also illustrates the locations of nine electrode penetrations within the dark, nonorientation-selective V2 thin stripe. This region was further characterized as a thin stripe on the basis of its preferential activation to isoluminant red-green gratings compared with luminance contrast stimuli (not shown) and its clearly defined hue map (see Xiao et al. 2003). The locations of these nine penetrations relative to the color-coded, statistically significant peak (75%) optical hue response contours are illustrated in Fig. 2*A* and relative to the vector-based hue response map in Fig. 2*B*. Five of these penetrations were located within the statistically significant peak hue response contours (penetrations C, F, G, H, and I), two were located just outside the peak response contours (penetrations D and E), and two penetrations were located further outside of the contours, but still within the nonoriented, color-preferring thin stripe (penetrations A and B).

The five penetrations within the statistically significant peak hue response map contained single neurons or multiunit recording sites with highly selective, consistent hue responses (Fig. 2*C*). In penetration G, the first neuron gave robust responses from orange to purple that resulted in a preferred angle of 84.54° and a color vector magnitude of 0.306. The next multiunit recording site was highly selective to orange, resulting in a preferred angle of 76.41° with a bias of 0.744. The third site in this penetration was a single cell that was slightly more broadly tuned, but it had a similar preference for

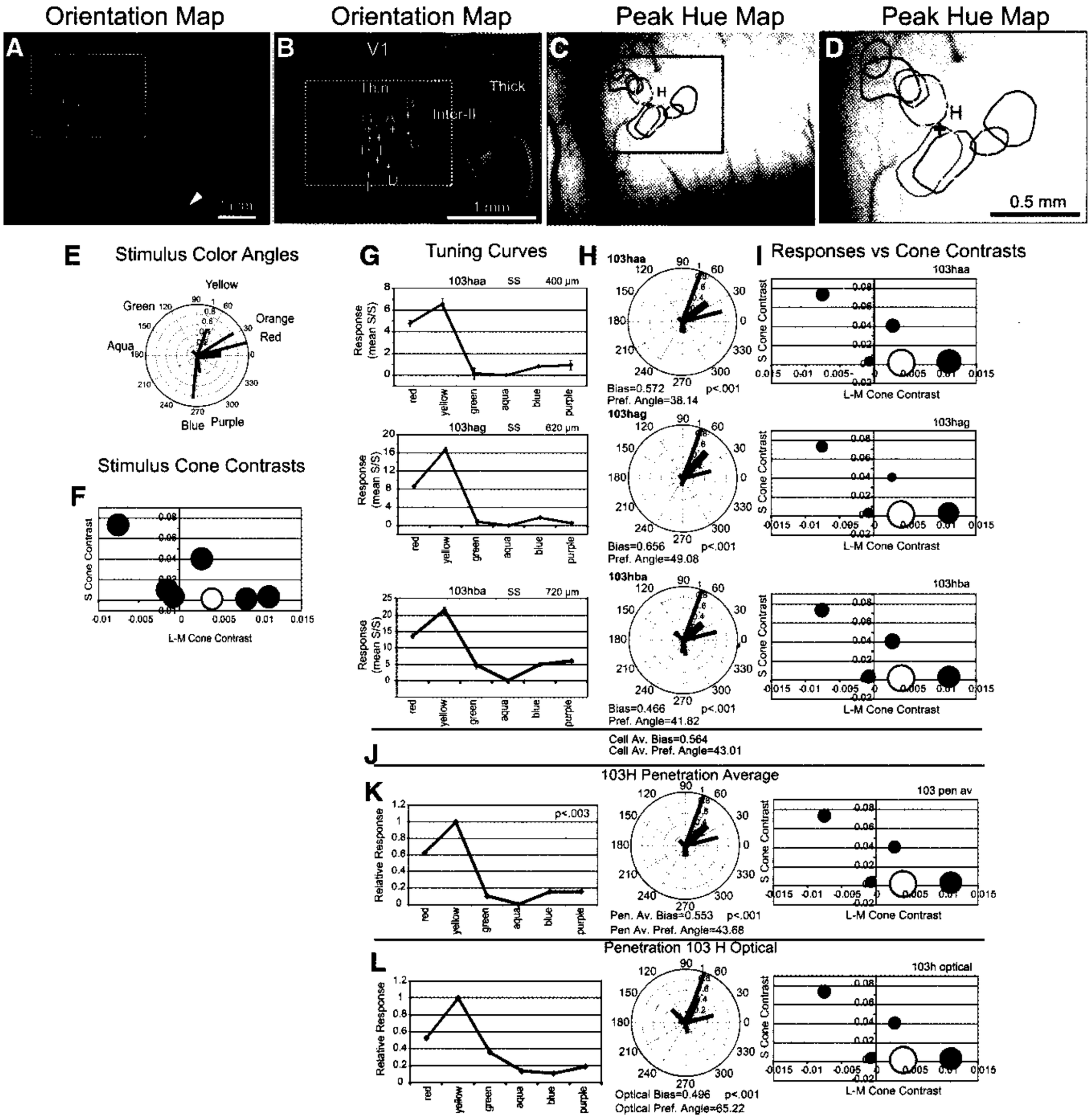

yellow with a preferred color vector angle of 99.06° with a magnitude of 0.432. The penetration average response, summarized in Fig. 2*E* (*bottom polar plot*), demonstrated a preferred color angle of 87.22° and a color vector magnitude of 0.450. Comparison of the average of the individual cell's vector bias (0.494) with the penetration average bias (0.450) with nearly identical preferred color angles (86.67 vs. 87.22°) indicates that the penetration and cell averages were nearly identical.

Penetration H was located within the yellow, statistically significant peak response domain and contained three single units that were highly selective for yellow-orange isoluminant stimuli. The summed color vectors for these three single cells displayed preferred color angles of 38.14, 49.08, and 41.82°, respectively. These cells were also highly selective for these resultant hues, with vector magnitudes of 0.572, 0.656, and 0.466, respectively. The penetration average response was highly selective (bias = 0.553) for yellowish-orange hues (preferred angle = 43.68°). The cell average and average penetration biases (0.564 vs. 0.553) and preferred angles (43.01 vs. 43.68°) were nearly identical, thus indicating the consistency of hue preference and selectivity within this penetration.

Penetration I was located within the statistically significant peak red hue domain and contained one multiunit and two single-unit recording sites that were highly selective for red hues (biases = 0.383, 0.481, and 0.540). The preferred color angles for these three recording sites ranged from 37.68° (orange) to 353.89° (deep red-purple). The penetration average vector had a preferred angle of 18.82° and vector magnitude of 0.438, indicating a high degree of selectivity for red stimuli. In addition, like penetration H, the cell average and penetration average biases (0.468 vs. 0.438) and color angles (18.41 vs. 18.82°) were nearly identical, further demonstrating the consistency of hue selectivity and hue preference within this penetration. Finally, penetrations C and F were located with the blue and yellow peak hue response domains, but only one recording site was tested in each, so penetration and cell average statistics could not be calculated.

Penetrations D and E were located immediately outside of the peak hue response domains and their constituent neurons displayed reduced hue selectivity compared with that of the previous four penetrations. In penetration D, two multiunit recording sites exhibited moderate to robust responses across a wide range of hues that resulted in color vector magnitudes of 0.065 and 0.123, respectively. These small, nonselective response vectors had preferred angles of 303.00 and 8.68°, respectively. The penetration average tuning was similarly broad, with a bias of 0.079 and a preferred angle of 345.32°. In penetration E, the two recorded single units had widely differing hue selectivity (bias = 0.034 and 0.450) and had widely differing preferred color angles of 128.90 and 261.42°. The resulting penetration average tuning curve reflected the differing preferred angles of the two recorded neurons with an intermediate preferred angle of 254.05° and an intermediate bias of 0.137. Thus in this penetration, the variability of preferred color angle (hue) resulted in a roughly 50% reduction in the penetration average color vector magnitude compared with the average cell color vector magnitude of 0.267.

Penetrations A and B were located further outside of the peak hue response domain, yet were located within the nonorientation-selective thin stripe (see Fig. 1*B*). Penetration A contained three single units that exhibited weak hue selectivity. The first two units exhibited the least hue selectivity in this penetration (bias = 0.162 and 0.175) and their preferred angles were largely similar (92.84 and 96.18°; yellow-green). The third cell was the most selective for hue and exhibited a color vector magnitude of 0.265, with a preferred color angle of 78.59° (yellow). The cell and penetration average responses were weakly selective for hue (bias = 0.200 vs. 0.196), with preferred color angles of 89.20 versus 87.89°. Thus the penetration average tuning simply reflected the broad tuning of individual cells that preferred yellow to yellow-green. In penetration B, a total of four recording sites were tested, with the first one reflecting multiunit activity and the next three reflecting single-unit activity. These four recording sites were nonselective for hue, with individual hue vectors of 0.051, 0.138, 0.056, and 0.067, respectively. The penetration average hue selectivity was also negligible (0.029), reflecting the lack of selectivity of individual recording sites and the variability (25.84 to 209.41°) of preferred color angles. Overall, these results suggest that robust hue selectivity and their clustering within a penetration are found only within the statistically significant peak hue response domains of V2 thin stripes.

FIG. 1. Hue selectivity in a single thin stripe penetration. *A*: low-magnification, color-coded orientation map centered on visual area 2 (V2) just posterior to the lunate sulcus. The white outline indicates the region reproduced at higher magnification illustrated in *B*. *B*: color-coded map illustrating the representation of orientation in area V2. The vector summation of single-condition responses to 4 different orientations was calculated for each pixel. The assigned color indicates the pixel preferred orientation and the pixel brightness indicates the magnitude of orientation selectivity. Bright orientation maps are observed in V2 thick and interstripe type II that are located to the *right* of the dark region of low orientation selectivity corresponding to the V2 thin stripe. The crosses and letters refer to electrode penetrations directed within the V2 thin stripe. *C*: color-coded, statistically significant ($P < 0.005$) peak (>75%) hue response contours calculated from the single-condition optical responses to each tested isoluminant hue. *D*: higher-magnification view of the peak hue map from the black outlined box in *C*, indicating the locations of electrode penetration H. *E*: polar representation of stimulus color angles and an example of single-hue responses (black) and resultant summed vector (red), indicating preferred hue (4.28°; red) and vector magnitude (hue selectivity, 0.46). *F*: bubble plot of L-M cone vs. S-cone contrast values of the 7 hue stimuli used in these experiments. *G*: conventional tuning curves of net firing rate response means and SEs as a function of hue for 3 single units recorded within 720 μm of the cortical surface. *H*: polar plots of single-hue responses (black vectors) and summed vectors (red) for 3 single-unit recording sites in this penetration. These cells were highly selective for hue (vector magnitudes of 0.572, 0.656, and 0.466) and shared very similar preferred color angles (38.14, 49.08, and 41.82°). *I*: normalized hue responses represented as a function of L-M vs. S-cone contrasts. The area of each circle represents the relative response compared with the hue generating the maximum response. *J*: average cell color vector magnitude and preferred color angle calculated across the 3 cells in this penetration. *K*: penetration average responses represented as conventional tuning curve (*left*), polar representation of hue response vectors and summed vector (*middle*), and relative response as a function of cone contrasts (*right*). The penetration average response was highly selective for hue (bias = 0.553) and preferred a color angle of 43.68° (orange). *L*: optical response calculated within a 210 × 210 μm region of interest (ROI) centered on the point of electrode penetration. Only 6 hues were tested (orange not tested) and the summed vector is highly selective (bias = 0.496) with a preferred color angle of 65.22° (yellow-orange). Overall, there is a high degree of consistency between the neuronal and optical estimates of hue preference and hue selectivity.

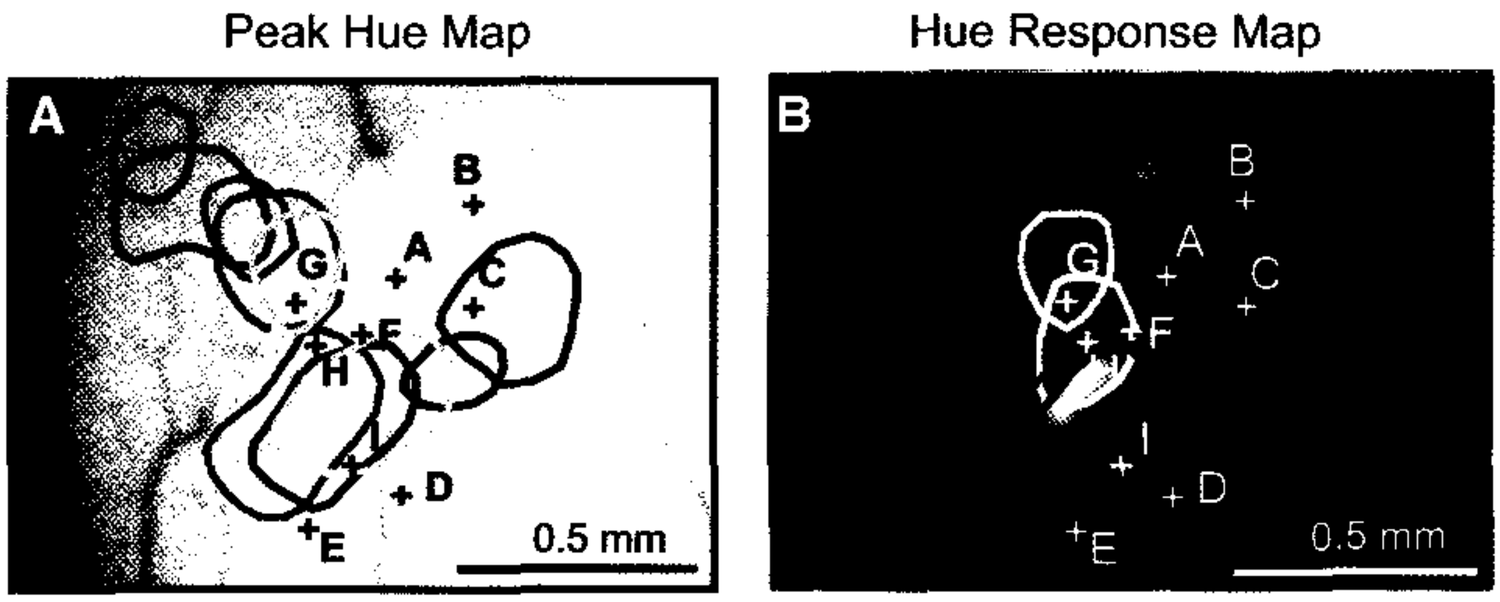

FIG. 2. Optical and electrophysiological analysis of hue selectivity. *A*: high-magnification view of the cortical surface indicating the location of 5 penetrations within the peak hue response map (penetrations C, F, G, H, and I) and 4 penetrations outside the peak hue map (penetrations A, B, D, and E). *B*: locations of the electrode penetrations and statistically significant peak hue response contours projected onto the color-coded hue response map. *C*: polar plots of electrophysiological responses to isoluminant hues for 5 penetrations within the peak hue map (*left*) and 4 penetrations just outside the peak hue map (*right*). Hue selectivity and preferred color angle are indicated for each recording site. Single (S) or multiunit (M) recordings and stationary (S) or moving (M) stimuli are indicated by the abbreviations SS, SM, MS, and MM. *D*: average color vector magnitude and preferred color angle across individual recording sites in each penetration. *E*: penetration average polar plots, hue selectivity (bias), and preferred color angle (hue) calculated by averaging the responses of individual hues across all cells in the penetration, normalizing the responses (black vectors), and then calculating the average color vector (red vector). *F*: polar plots illustrating the results of the ROI analysis (210 × 210 μm) of single-condition responses from intrinsic optical imaging of responses to isoluminant hues. Case m0103.

Intrinsic optical imaging analysis of V2 thin stripe hue selectivity

The color vector-summation method provides a common means to compare the chromatic tuning of single cells or multiunit activity, average neuronal selectivity within a penetration, and local population hue selectivity as measured by intrinsic signal cortical imaging. For the analysis of intrinsic optical images, a 210 × 210 μm ROI was centered at the location of each electrode penetration and average pixel single-condition responses were summed vectorially to yield a color vector whose angle indicated the preferred hue within the ROI and whose magnitude indicated the degree of hue selectivity. An example of optically defined hue preference and selectivity is illustrated for the ROI centered on penetration 103H in Fig. 1*L*. In this case, there is a high degree of correspondence between the penetration average and optical ROI estimates of preferred hue and hue selectivity (see following text).

CASE M0103. The optically defined color selectivity from case m0103 is summarized below each penetration average hue vector plot (Fig. 2*F*). The ROIs associated with penetrations G, H, I, F, and C demonstrated high to moderate degrees of hue selectivity on the basis of their color vector magnitudes of 0.609, 0.496, 0.229, 0.423, and 0.182, respectively. The penetration average neuronal response observed in penetration G (Fig. 2*E*) exhibited a high degree of hue selectivity (bias = 0.450) for a preferred color angle of 87.22° (yellow-green), but the corresponding optical response was even more highly selective (bias = 0.607) and exhibited a preference for green stimuli (color angle, 135.95°). The penetration average and optical responses associated with penetration H were similar in the degree of their hue selectivity (bias = 0.553 and 0.496, respectively) and preferred color angles (43.68 and 65.22°, respectively) and were in excellent agreement with their position within the yellow and orange peak response contours of the hue map. A similar degree of correspondence between the electrophysiological and optical ROI estimates of hue selectivity was observed for penetration I that was located within the red and orange significant peak hue response contours. Here, the penetration average hue selectivity (0.438) was greater than the optically defined hue selectivity (0.229), which is in agreement with the population as a whole (see following text). In addition, the estimates of preferred color angle were highly similar due to their peak responses to red, but the penetration average had slightly greater responses to yellow stimuli, resulting in a preferred angle of 18.82° (red), whereas the preferred optical color angle was 2.86° (red), attributed largely to the weaker responses to yellow.

Since penetrations F and C contained only one recording site each, comparisons between cell and optical responses are somewhat limited in their interpretation. In penetration F, the cell and optic preferred color angles were dissimilar (237.41 vs. 35.05°) and the optical responses were more highly selective (0.423) than the single-cell color vector bias (0.138). The single-cell and optical analyses for penetration C were highly consistent in preferred color angle (257.26 and 239.16°, respectively). However, in contrast to penetration F, the estimate of hue selectivity was greater for the single recording site (0.472) than that for the optical response (0.182), largely reflecting the greater optical responses to green and aqua.

Penetrations A, B, D, and E were located outside of the peak response hue map and the optical and penetration average estimates of hue selectivity were largely similar to each other and were smaller in magnitude than those observed in the penetrations within the peak hue response map. In each of these penetrations, electrophysiological and optical responses were generally observed across a wide range of hues, resulting in penetration average and optically defined color vector magnitude pairs of A = 0.196: 0.138; B = 0.029: 0.106; D = 0.079: 0.183; and E = 0.137: 0.236. The penetration average and optical preferred color angles were somewhat similar to each other, but differed on average by about 78°. This result is not surprising given the small magnitude of the resultant color vectors.

CASE M005. Locations of the four electrode penetrations from case m005 are illustrated on the cortical surface in Fig. 3*A*. This panel also illustrates the spatial organization of the statistically significant ($P < 0.005$) peak hue response map contours derived from intrinsic cortical imaging. This hue map was located in a portion of V2 preferentially activated by isoluminant compared with luminance-contrast stimuli (red/green-luminance; not shown) that was largely devoid of orientation-selective responses (Fig. 3*B*). Locations of these four penetrations relative to the optically defined hue map defined from the vector summation of seven isoluminant hue responses are illustrated in Fig. 3*C* and at higher magnification in Fig. 3*D*. The average cell and penetration average statistics from this case are based on two single- and multiunit responses in penetration A, three from penetration B, five from penetration D, and seven from penetration E.

The average cell hue preference and selectivity from the four penetrations in case m005 are illustrated in Fig. 3*E*. The polar plots and calculated preferred hues and hue selectivity (color vector magnitude) for the electrophysiologically defined penetration average and optically defined ROIs are illustrated in Fig. 3, *F* and *G*, respectively. Penetration A was located within the red peak response contour and its penetration average hue response was highly selective for red, demonstrating a preferred color angle of 24.85° and a color vector magnitude of 0.612. The optical ROI analysis revealed a strikingly similar high degree of hue selectivity (bias = 0.575) and a nearly identical preference for red (color angle = 23.68°).

Penetration C was located within the green peak response contour of the optical map and abutted the aqua contour. The penetration average electrophysiological response exhibited a broad range of responses to blue, yellow, orange, and red that resulted in a moderate degree of hue selectivity (bias = 0.273) for the preferred color angle of 27.73°. The corresponding optical ROI analysis demonstrated a higher degree of hue selectivity (bias = 0.452) for the preferred color angle of 150.82° (aqua). This discrepancy between the electrophysiological and optical ROI estimates of hue selectivity appears largely due to robust electrophysiological responses to red, orange, and yellow, not observed in this portion of the optical map.

Penetration D was located within the blue and purple statistically significant peak response contours and the penetration average exhibited robust responses to blue and red, with weaker responses to orange, yellow, aqua, and purple. The resultant summed vector displayed high selectivity (color vec-

tor magnitude of 0.323) for its preferred color angle of 349.40°. The optical ROI-derived responses were very similar to the electrophysiological penetration average, exhibiting a preferred color angle of 291.41° and a color vector magnitude of 0.359. Penetration E was located within the green peak response contour and its penetration average response demonstrated a high degree of selectivity (bias = 0.441) for its preferred color angle of 15.72°. This penetration average response reflects the consistent robust responses to blue and red and weaker responses to orange and yellow. The optical ROI-defined responses were also highly selective for hue (bias = 0.384), but differed substantially from the electrophysiological penetration average tuning in preferred color angle (162.50°). Similar to penetration C, this difference in preferred color angle appears to be due largely to increased neuronal responses to red and yellow and relatively greater optical responses to green and aqua.

CASE W13. In case w13 four penetrations were directed at a V2 thin stripe, defined by its location between orientation-selective responses in V2 thick/interstripes (Fig. 3*H*), by its preferential activation to red-green isoluminant color stimuli compared with luminance-contrast stimuli (Fig. 3*I*) and by the presence of a spatially organized hue map (Fig. 3, *J* and *K*). The locations of these four penetrations, relative to the optically defined hue map, are illustrated in Fig. 3*J* and at higher magnification in Fig. 3*K*. Penetrations D and E each contained two single-unit recording sites that were centered within the statistically significant peak response domain of the hue map. In contrast, penetrations A and B were located just outside of the peak hue map and each contained two single-unit recording sites. The electrophysiological penetration average response from penetration A revealed a small color bias (0.184) for orange (color angle = 37.94°). The optical ROI-defined color tuning revealed a preference for yellow-orange (color angle = 60.29°) and a similar weak color bias (0.195), thus demonstrating a high degree of similarity with the neuronal hue tuning. The narrowly tuned penetration average responses from penetration B resulted in a large summed vector magnitude (0.393) that indicated a preferred color angle of 22.42°. Similar to penetration A, the optical tuning for hue in penetration B was broad, but the resultant summed vector revealed a moderate color vector magnitude of 0.287 and a preferred color angle of 49.81°.

In contrast to penetrations A and B, the two penetrations located within the peak hue map demonstrated robust hue selectivity in both the electrophysiologically defined penetration average and optical ROI-defined analyses. Penetration D was located within the yellow-orange domain of the peak hue map and the corresponding penetration average tuning reflected a high degree of hue selectivity (bias = 0.490) for the preferred color angle of 351.62° (red). The optical ROI-defined hue responses exhibited a nearly identical high degree of hue selectivity (bias = 0.483) for a preferred color angle of 37.93° (orange). Although peak electrophysiological and optical responses were observed to red stimuli, the difference between the penetration average and optical hue tuning appeared to be due largely to the more robust optical responses to yellow and green and a slightly weaker response to blue stimuli. Penetration E was located within the red-orange domain of the peak hue map and the penetration average tuning reflected a high degree of selectivity (bias = 0.384) for a color angle of 49.50° (orange-yellow). The optical ROI-defined responses exhibited a very similar high degree of hue selectivity (bias = 0.401) for a similar preferred color angle of 38.04° (orange).

Hue selectivity varies across different V2 thin stripe submodules

In the current experiments, hue selectivity was examined both within the statistically significant peak response domains of V2 thin stripe hue maps and within the thin stripe region immediately outside these hue maps. In this section, the average hue selectivities of these two subregions of V2 thin stripes are compared using the color vector magnitudes from the ROI analysis of intrinsic optical imaging, the penetration average color vector magnitude, and the average color vector magnitude of individual single-unit and multiunit recording sites within each penetration. The average color vector magnitudes for penetrations inside and immediately outside of the peak hue maps are illustrated for these three different methods in Fig. 4*A*, which illustrates that average color vector magnitude (hue selectivity) is large within the peak response hue maps and differs significantly from that observed just outside the map. This difference is observed in the average vector magnitudes determined with optical recording (0.430_{in} vs. 0.191_{out}, $t = 4.96_{2\ tail}$; $P < 0.000026$), penetration average color vector magnitude (0.440_{in} vs. 0.170_{out}, $t = 4.33_{2\ tail}$; $P < 0.0019$), and average cell color vector magnitude (0.498_{in} vs. 0.251_{out}, $t = 3.33_{2\ tail}$; $P < 0.0125$). Since thin stripes encompass the peak hue response maps and the immediately adjacent regions, these results demonstrate that hue selectivity varies considerably within V2 thin stripes. Furthermore, since penetrations defined as inside and outside of the peak hue maps were separated by distances of 200–300 μm, small positional changes within thin stripes can have a profound, statistically significant effect on the magnitude of the observed hue selectivity. This functional heterogeneity within V2 thin stripes may be due to the parallel organization of luminance-change domains (Wang et al. 2007) and may account for some of the observed variability in previous reports of the prevalence of color selectivity in thin stripes.

Intrinsic optical imaging and electrophysiological analyses of hue selectivity compared

The ability of intrinsic optical imaging to predict the magnitude of penetration average neuronal hue selectivity is summarized in Fig. 4*B*. For this analysis, the intrinsic optical ROI analysis of color vector magnitude (hue selectivity) was compared with the penetration average color vector magnitudes for the corresponding 15 microelectrode penetrations. The resultant statistically significant linear regression ($P < 0.00007$) indicates that more than two thirds of the experimental variance is accounted for by the linear regression ($y = 0.753x + 0.084$; $r^2 = 0.718$). A similar relationship is also found between optical ROI estimates of hue selectivity and cell average color vector magnitudes within the association electrode penetrations (not shown; $y = 0.787x + 0.140$, $r^2 = 0.533$, $P < 0.009$). These results demonstrate that intrinsic cortical imaging estimates of hue selectivity in V2 thin stripes are highly correlated with the spiking activity of the constituent neurons.

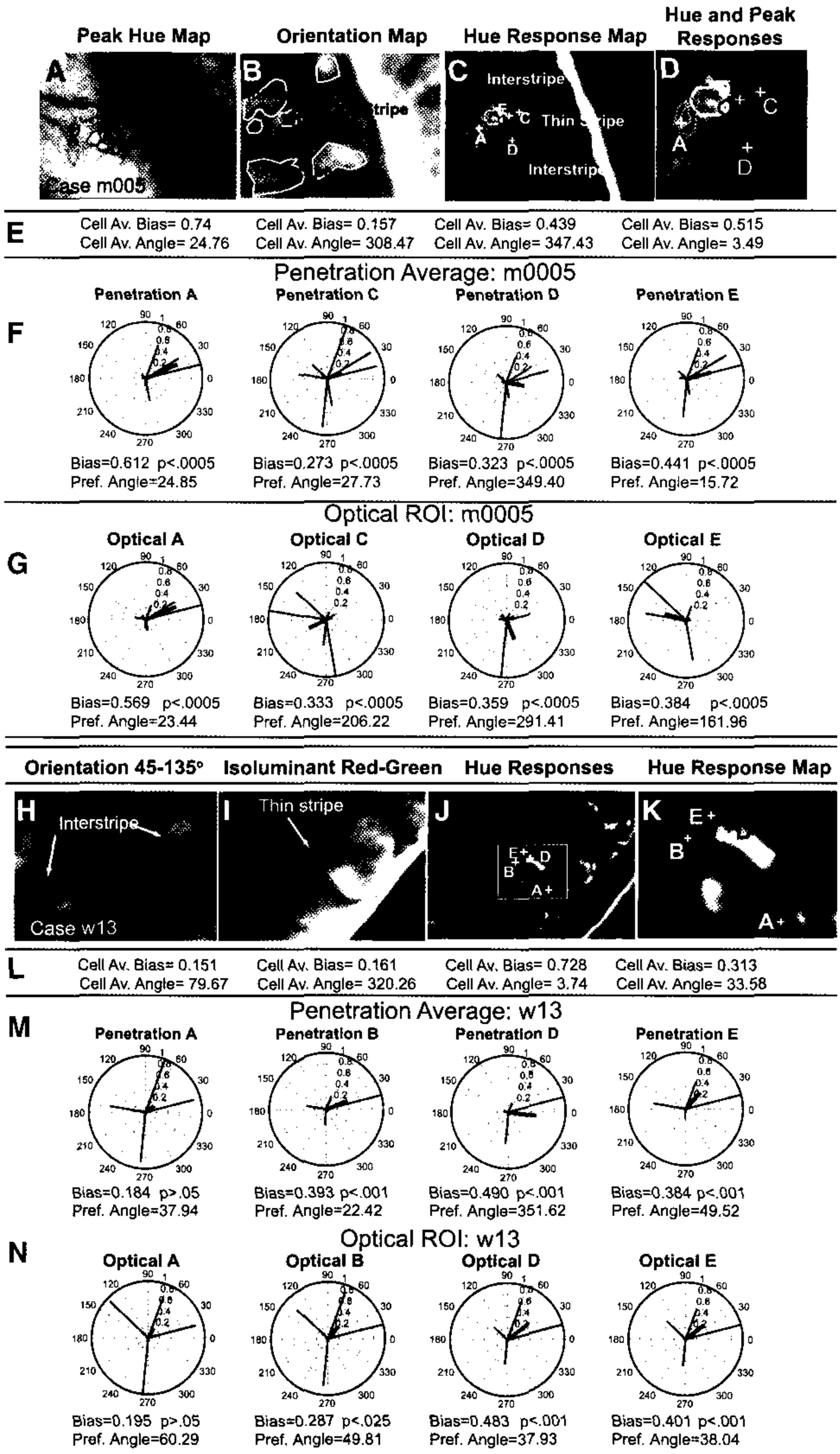

FIG. 3. Penetration average and optical analysis of hue selectivity in relation to the peak hue map. *A*: location of 4 electrode penetrations relative to the statistically significant peak hue response contours as projected onto the cortical surface in case m005. *B*: electrode penetrations and peak hue response contours projected onto differential image of orientation preference (45–135°), demonstrating orientation-selective domains located just outside of the peak hue map. *C*: electrode penetrations and peak hue response contours projected onto the optically determined, vector-based, hue response map. *D*: close-up of *C* indicating the positions of electrode penetrations relative to the vector-based hue response map. *E*: average color vector magnitude and preferred color angle for 2–5 single- or multiunit recording sites in each penetration. *F*: penetration average polar plots of hue selectivity (bias) and preferred color angle (hue). The red vector indicates the calculated preferred hue and its length indicates the degree of hue selectivity. *G*: polar plots illustrating the results of the ROI analysis of single-condition responses from intrinsic optical imaging of responses to isoluminant hues. *H*: differential image of orientation responses (45–135°), demonstrating orientation-selective activity in V2 interstripes flanking a V2 thin stripe in case w13. *I*: differential image of isoluminant color activations (red-green), demonstrating the color-preferring domain of this V2 thin stripe. *J*: low-magnification view of the positions of 4 recording sites projected onto the hue response map based on vector summation of isoluminant hue responses. *K*: high-magnification view of 4 recording sites projected onto the vector-based hue response map from the white box in *J*. Penetrations A and B were located in regions of low color selectivity, whereas penetrations D and E were located in regions of high color selectivity (large color vector magnitude). *L*: average hue selectivity (bias) and average preferred hue (color vector angle) calculated across 2–5 recording sites in each penetration. *M*: polar representation of penetration average hue responses (black vectors) and summed vector (red), indicating the preferred hue (vector angle) and magnitude of hue selectivity (color vector magnitude or bias). *N*: polar plots illustrating the results of the ROI analysis of single-condition responses from intrinsic optical imaging of responses to isoluminant hues.

It remains to be determined whether other functional measurements of neural activity, such as local field potentials (LFPs), are more highly correlated with the optical signal or account for additional variance not contained within the neuronal spiking activity.

The relationship between the electrophysiological and optical ROI-derived estimates of preferred hue was determined using circular correlation of their preferred color angles (Mardia and Jupp 2000). This analysis indicated that optical and penetration average estimates of preferred hue (color angle)

were significantly correlated (circular correlation: $r_c = 0.507$; $Z_{r\_c} = 1.668$, $P < 0.045$). The difference between neuronal penetration average and intrinsic optical estimates of preferred color angle is summarized in Fig. 4*C*. In this figure, each bar illustrates the difference in optically and electrophysiologically defined preferred color angles. The nine bars on the *left* represent penetrations located within the peak hue maps, whereas the six bars on the *right* are from penetrations outside of the peak hue map. On average, the optical and penetration average estimates of preferred color angle differ by 59.75° and the penetrations inside and outside of the peak hue map do not differ in their color angle differences ($P > 0.992$). The large average preferred angle difference for penetrations within the peak hue map is due mainly to penetrations m0005c and m0005e. Although it remains uncertain why only these two *penetrations showed such striking differences in cell and optical* preferred color angles, it is worthwhile identifying some of possible contributing factors. First, it is striking that the angle differences in penetration E reflect different phases of a conventional color-opponent response. Perhaps the optical responses integrated across both ON and OFF responses, whereas only the ON phases of the cell data were analyzed. Second, the optical responses tend to be more widely distributed across color angles and thus responses near blue, aqua, and green may shift the preferred color angle away from the large red response. The observed color angle differences may also be partially attributed to small targeting errors (~100 μm) that can result in large deviations from the optical preferred color angles. Finally, since the final electrophysiological recording session was conducted 2 weeks after the optical hue map was recorded, small changes in cortical curvature or plastic changes in cortical maps may have contributed to the mismatch observed *in these last two penetrations of the experiment. If these* two penetrations were excluded, the preferred angle differences between penetrations inside and outside of the peak hue map are statistically significant (one-tail *t*-test, $P > 0.045$).

The relationship between penetration average neuronal responses and optical responses derived from the ROI analyses was explored further using a traditional technique not based on the vector-summation method described earlier. In this analysis, the average electrophysiological responses were normalized within each penetration and were compared with the normalized optical responses within the ROI associated with

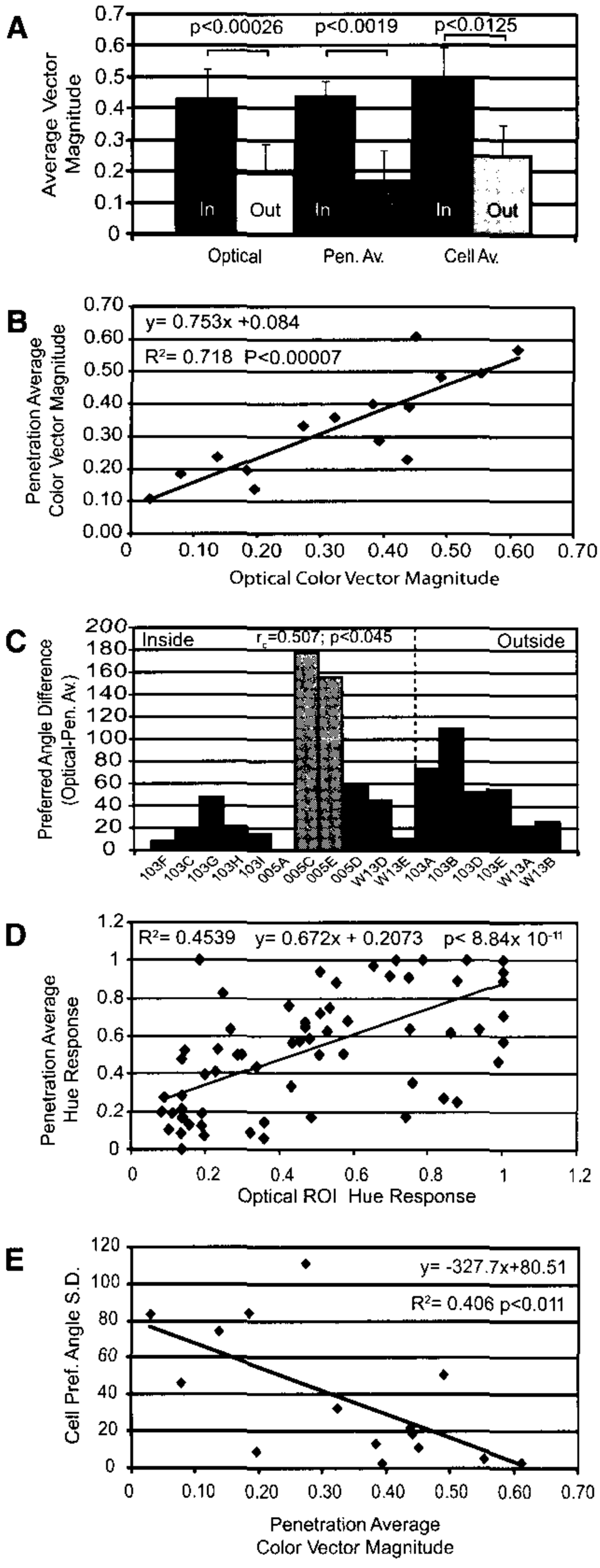

FIG. 4. Analysis of optical and electrophysiological hue selectivity. *A*: comparison of color vector response magnitudes (hue selectivity) inside vs. outside the statistically significant peak hue response map based on ROI analysis of optical responses ($P < 0.00026$), penetration average neuronal responses ($P < 0.0019$), and average neuronal responses ($P < 0.0125$). *B*: relationship between color vector magnitudes (hue selectivity) as determined through ROI analysis of optical responses and penetration average neuronal responses. The resultant correlation is strong ($r^2 = 0.718$) and highly significant ($P < 0.00007$). *C*: bar graph illustrating the difference in preferred color angles for penetration average neuronal responses and ROI analyses of optical responses across all penetrations. The 9 bars on the *left* represent penetrations inside the peak hue map, whereas the 6 bars on the *right* represent penetrations outside of the peak hue map. The calculated preferred color angles are highly similar and statistically significant (circular correlation; $r_c = 0.507$, $Z_{r\_c} = 1.668$; $P < 0.045$). *D*: relationship between normalized optical ROI responses and electrophysiological penetration average responses for each stimulus condition across 15 of 17 penetrations. The resultant correlation is highly significant ($r^2 = 0.4539$, $P < 8.84 \times 10^{-11}$). Penetrations 005c and 005e were excluded due to their weakly modulated responses and their strong negative correlations (see *C*). The overall correlation is still highly significant if all 17 penetrations are included ($r^2 = -0.1714$, $P < 0.000742$). *E*: relationship between penetration average hue selectivity (color vector magnitude) and the SD of individual cell's preferred hue (color vector angle). This relationship is significant ($P < 0.011$ and $r^2 = 0.406$), indicating that recording sites from penetrations with high hue selectivity have little variability in their preferred hues, whereas penetrations with low hue selectivity have a high degree of variability in their cell's preferred hues.

each penetration. Thus a linear regression was calculated that compared the normalized neuronal and optical responses generated for each stimulus condition across all penetrations. This relationship is illustrated in Fig. 4*D* for 15 penetrations (penetrations 005c and 005e excluded; see preceding text). The overall linear regression is highly significant ($r^2 = 0.4539$; $P < 8.84 \times 10^{-11}$) and demonstrates that the optical responses slightly underestimate the neuronal responses. Penetrations 005c and 005e were excluded from this illustration since their neuronal to optical regression had a strong negative slope and yielded significant mismatches in preferred hues. Nevertheless, if these two penetrations were included in the overall assessment of the neuronal and optical response regression, the resultant function would still be highly significant ($r^2 = 0.1714$; $P < 7.42 \times 10^{-5}$).

Columnar organization of hue in V2 thin stripe hue maps

The results indicate that the ROI analysis of intrinsic signal optical imaging provides a reliable predictor of the average hue preference and hue selectivity within a cortical column in a thin stripe. In this section, the relationship between the preferred hues (color angles) of individual neurons (or multiunit recording sites) and the penetration average hue selectivity is examined to better understand the columnar organization of hue. Figure 4*D* illustrates the relationship between penetration average color vector magnitude (hue selectivity) and the SD of preferred color angles within each penetration. The results indicate that the variance of preferred hues (color angles) across individual cells (or multiunit recording sites) within a penetration is negatively correlated with the penetration average color vector magnitude ($P < 0.011$). Thus low penetration average hue selectivity is associated with high color angle variance, whereas high penetration hue selectivity is associated with small color angle variance. Furthermore, the regression equation ($y = -327.7x + 80.51$; $r^2 = 0.406$) demonstrates that more than one third of the experimental variance is accounted for by this simple linear relationship. Overall, these results demonstrate that penetrations that are highly selective for hue contain neurons that are both individually hue selective and are selective for the similar hues.

DISCUSSION

Functional architecture of V2

Intrinsic optical recording studies have consistently emphasized the differences between V2 stripe compartments. Thick stripes and interstripes have been consistently found to contain an orderly representation of orientation that is clearly lacking in thin stripes (e.g., Roe and Ts'o 1995; Ts'o et al. 2001; Wang et al. 2007; Xiao et al. 2003). Thick stripes also contain representations of binocular disparity that are lacking in both thin stripes and interstripes (Chen et al. 2008). Conversely, thin stripes contain orderly representations of hue and luminance change that are lacking in both thick stripes and interstripes (Lu and Roe 1908; Wang et al. 2007; Xiao et al. 2003). At face value, these results are inconsistent with some previous electrophysiological findings that demonstrated a substantial homogeneity of response properties of individual neurons across these three stripe compartments. This apparent mismatch may be best explained by considering not only the percentage of neurons in each stripe compartment demonstrating selectivity for a given stimulus feature, but also how those selective neurons are organized into cortical columns and the horizontal distribution of selective neurons within each compartment. Since intrinsic optical imaging measures a hemodynamic response of a population of neural elements, the present results suggest that the constituent neural populations are organized according to orientation in thick stripes and interstripes, disparity in thick stripes, and hue (and luminance change) in thin stripes.

The organization of preferred hue and hue selectivity revealed in the current experiments are schematically illustrated in Fig. 5. The results demonstrate that V2 thin stripes contain regions that differ in their selectivity for stimulus hue. Portions of V2 thin stripes that are located within the statistically significant peak response domains exhibit moderate to large summed color response vector magnitudes, characteristic of highly selective responses to hue. Individual neurons in these regions are highly selective for hue and are organized into columns that share similar preferred hues. Our findings demonstrate that cell preferences for a common hue, in conjunction with a high degree of hue selectivity, result in a penetration average tuning that is also highly selective for the same hue.

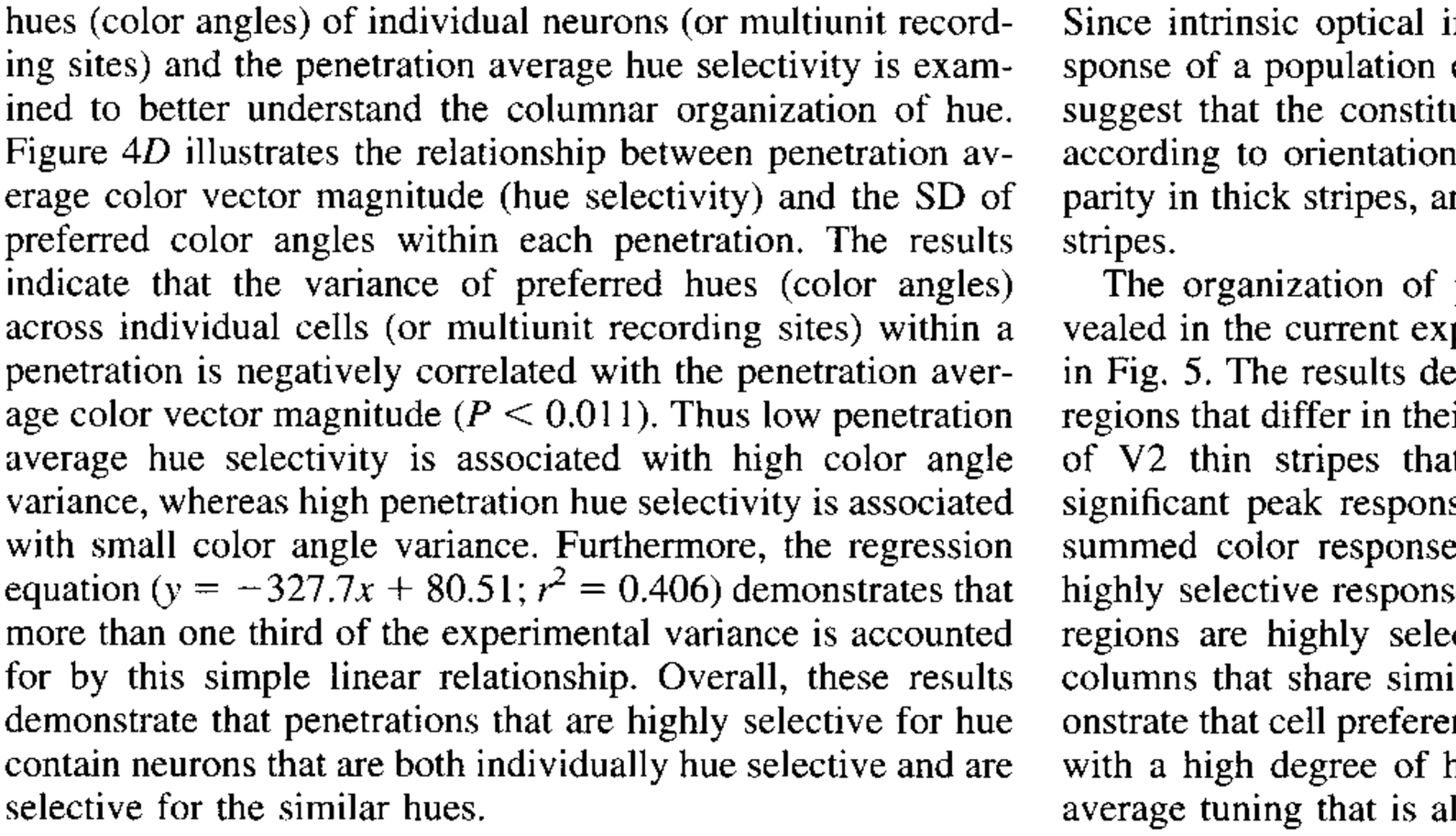

FIG. 5. Schematic representation of hue preference and selectivity in V2 thin stripes. In this model of hue selectivity in V2 thin stripes neurons encountered in electrode penetrations within the statistically significant peak hue maps tend to exhibit robust hue selectivity (larger circles at recording site). Furthermore, neurons within these penetrations tend to prefer the same or similar hues. In contrast, neurons encountered in penetrations outside of the peak hue map tend to exhibit weak or no hue selectivity (small circles) and the calculated preferred hues are more variable from cell to cell.

Immediately outside of the statistically significant peak hue map, there is a clear reduction in hue selectivity in individual neurons, penetration average responses, and optical responses. These nonselective penetrations are nonetheless located within V2 thin stripes and most likely constitute portions of the luminance-change module system (Roe and Ts'o 1995; Wang et al. 2007; Xiao et al. 2003). This functional heterogeneity within V2 thin stripes may partially account for the variability in the proportion of thin stripe neurons reported to be selective for color (e.g., DeYoe and Van Essen 1985, 86%; Gegenfurtner et al. 1996, 50%; Levitt et al. 1994, 25%). Since V2 thin stripes have been reported to contain a substantial proportion of orientation-selective neurons, the lack of an orientation map in thin stripes may be due to the disordered organization of preferred orientation rather than simply due to a lack of selective neurons (DeYoe and Van Essen 1985, 20%; Gegenfurtner et al. 1996, 72%; Levitt et al. 1994, 50%; Peterhans and von der Heydt 1993, 65%).

The precise organization of hue selectivity in V2 thin stripes most likely arises from highly specific hue-selective inputs from V1. V1 contains an array of hue maps that are smaller than those in V2 (~200 μm vs. ~1 mm) (Chatterjee et al. 2008; Xiao et al. 2007). These hue maps appear to be colocalized with CO blobs in V1 (Chatterjee et al. 2008; Lu and Roe 2008; Xiao et al. 2007). Compared with interblob regions, V1 blobs contain a higher concentration of cells that project to V2 thin stripes (Sincich and Horton 2005; Xiao and Felleman 2004), suggesting that the hue-specific organization in V2 thin stripes originates from similar organization in V1 blobs.

Since V2 receptive fields are two- to fourfold larger than the corresponding V1 receptive fields (Gattas et al. 1981; Smith et al. 2001), V2 thin stripe hue maps appear to receive hue-specific, convergent input from a number of V1 blobs. This suggestion is consistent with the observation of wide divergence of nonoriented, color-specific projections from V1 blobs to V2 thin stripes observed using single-cell cross-correlation techniques (Roe and Ts'o 1999). The reduced hue selectivity found in V2 thin stripes, but outside of the peak hue maps, may be due to a greater intermixing of hue-specific inputs from V1 blobs, convergent input from weakly hue selective V1 neurons, or a combination of the two.

Neuronal basis of the intrinsic cortical signal

In these experiments, preferred hue and hue selectivity were determined from the same cortical regions using both intrinsic optical imaging and electrophysiological recording. This experimental design provided a unique opportunity to determine the degree to which the hemodynamic optical signal was correlated with the recorded neuronal responses. Although it is not possible to record activity from all neural elements that may contribute to the ROI-based optical signal, the present results suggest that the penetration average hue tuning is significantly correlated with the hue tuning observed in the intrinsic optical signal. In the current experiment, the color vector magnitude determined with optical recording is correlated with the penetration average vector magnitude with an r^2 value of 0.718, indicating that more than two thirds of the observed experimental variance is accounted for by the simple linear regression of these two variables. Similarly, across all penetrations, the optically defined color vector preferred hue (angle) is strongly correlated with the penetration average preferred angle with an r value of 0.507, indicating that one quarter of the variance is accounted for by the regression between these two circular variables. These results suggest that neuronal spiking activity accounts for a significant percentage of the recorded intrinsic optical signal. This interpretation is consistent with reports from the functional magnetic resonance literature that indicate the blood oxygenation level–dependent signal is correlated with neuronal spiking activity as well as with LFPs (e.g., Logothetis and Wandell 2004). Additional experimentation will be necessary to determine whether LFPs provide better estimates of the intrinsic signal in V2 or whether the combination of LFP and spiking activity provides a more comprehensive basis for the intrinsic optical signal.

ACKNOWLEDGMENTS

We thank Q. Huang for technical support and A. Zych and X. Huang for computer programming.

GRANTS

This research was supported by National Eye Institute Grants R01-EY-08372 and R01-EY-018897 to D. J. Felleman, a research grant from the Whitehall Foundation, a Vision Core Grant from the National Eye Institute to the University of Texas Health Science Center at Houston, and National Natural Science Foundation of China Grant 30623004 to Y. Wang.

REFERENCES

Batschelet E. *Circular Statistics in Biology*. New York: Academic Press, 1981.

Chatterjee S, Ohki K, Reid RC. Functional micro-architecture of color selectivity in macaque primary visual cortex. Program No. 666.15. *2008 Abstract Viewer/Itinerary*. Washington, DC: Society for Neuroscience, 2008. Online.

Chen G, Lu HD, Roe AW. A map for horizontal disparity in monkey V2. *Neuron* 58: 442–450, 2008.

Conway BR, Moeller S, Tsao DY. Specialized color modules in macaque extrastriate cortex. *Neuron* 56: 560–573, 2007.

DeYoe EA, Van Essen DC. Segregation of efferent connections and receptive field properties in visual area V2 of the macaque. *Nature* 317: 58–61, 1985.

Fisher NI. *Statistical Analysis of Circular Data*. New York: Cambridge Univ. Press, 1993.

Gattass R, Gross CG, Sandell JH. Visual topography of V2 in the macaque. *J Comp Neurol* 201: 519–539, 1981.

Gegenfurtner KR. Cortical mechanisms of colour vision. *Nat Rev Neurosci* 7: 563–572, 2003.

Gegenfurtner KR, Kiper DC, Fenstemaker SB. Processing of color, form, and motion in macaque area V2. *Vis Neurosci* 13: 161–172, 1996.

Hubel DH, Livingstone M. Segregation of form, color, and stereopsis in primate area 18. *J Neurosci* 7: 3378–3415, 1987.

Levick WR, Thibos LN. Analysis of orientation bias in cat retina. *J Physiol* 329: 243–261, 1982.

Levitt JB, Kiper DC, Movshon JA. Receptive fields and functional architecture of macaque V2. *J Neurophysiol* 71: 2517–2542, 1994.

Livingstone M, Hubel D. Segregation of form, color, movement and depth: anatomy, physiology, and perception. *Science* 240: 740–749, 1988.

Logothetis NK, Wandell BA. Interpreting the BOLD signal. *Annu Rev Physiol* 66: 735–769, 2004.

Lu HD, Roe AW. Functional organization of color domains in V1 and V2 of macaque monkey revealed by optical imaging. *Cereb Cortex* 18: 516–533, 2008.

Mardia KV, Jupp PE. *Directional Statistics*. New York: Wiley, 2000.

Peterhans E, von der Heydt R. Functional organization of area V2 in the alert monkey. *Eur J Neurosci* 5: 509–524, 1993.

Ratzlaff EH, Grinvald A. A tandem lens epifluorescence macroscope: hundred-fold brightness advantage for wide-field imaging. *J Neurosci Methods* 36: 127–137, 1991.

Roe AW, Ts'o DY. Visual topography in primate V2: multiple representations across functional stripes. *J Neurosci* 15: 3689–3715, 1995.

Roe AW, Ts'o DY. Specificity of color connectivity between primate V1 and V2. *J Neurophysiol* 82: 2719–2730, 1999.

Shipp S, Zeki S. The functional organization of area V2, I: Specialization across stripes and layers. *Vis Neurosci* 19: 187–210, 2002.

Shou T, Leventhal AG. Organized arrangement of orientation-selective relay cells in the cat's dorsal lateral geniculate nucleus. *J Neurosci* 9: 4287–4302, 1989.

Sincich LC, Horton JC. Input to V2 thin stripes arises from V1 cytochrome oxidase patches. *J Neurosci* 25: 10087–10093, 2005a.

Sincich LC, Horton JC. The circuitry of V1 and V2: integration of color, form, and motion. *Annu Rev Neurosci* 28: 303–326, 2005b.

Smith AT, Singh KD, Williams AL, Greenlee MW. Estimating receptive field size from fMRI data in human striate and extrastriate visual cortex. *Cereb Cortex* 11: 1182–1190, 2001.

Stockman A, Sharpe LT. The spectral sensitivities of the middle- and long-wavelength-sensitive cones derived from measurements in observers of known genotype. *Vision Res* 40: 1711–1737, 2000.

Swindale NV. Orientation tuning curves: empirical description and estimation of parameters. *Biol Cybern* 78: 45–56, 1998.

Ts'o DY, Roe AW, Gilbert CD. A hierarchy of the functional organization for color, form, and disparity in primate visual area V2. *Vision Res* 41: 1333–1349, 2001.

Wade AR, Rieger JW, Wandell BA. Functional measurements of human ventral occipital cortex: retinotopy and colour. *Philos Trans R Soc Lond B Biol Sci* 357: 963–973, 2002.

Wang Y, Xiao Y, Felleman DJ. V2 thin stripes contain spatially organized representation of luminance change. *Cereb Cortex* 17: 116–129, 2007.

Wyszecki G, Stiles WS. *Color Science* (2nd ed.). New York: Wiley, 1982.

Xiao Y, Casti A, Xiao J, Kaplan E. Hue maps in primate striate cortex. *NeuroImage* 35: 771–786, 2007.

Xiao Y, Felleman DJ. Projections from primary visual cortex to cytochrome oxidase thin stripes and interstripes of macaque visual area 2. *Proc Natl Acad Sci USA* 101: 7147–7151, 2004.

Xiao Y, Wang Y, Felleman DJ. A spatially organized representation of colour in macaque cortical area V2. *Nature* 421: 535–539, 2003.